Available online at www.sciencedirect.com

ScienceDirect

Journal of Ocean Engineering and Science 3 (2018) 295–302

www.elsevier.com/locate/joes

Original Article

New analytic solutions of the space-time fractional Broer–Kaup and approximate long water wave equations

H. Çerdik Yaslan

Department of Mathematics, Pamukkale University, Denizli 20070, Turkey

Received 29 April 2018; received in revised form 20 October 2018; accepted 20 October 2018
Available online 26 October 2018

Abstract

In the present paper, the $\exp(-\phi(\xi))$ expansion method is applied to the fractional Broer–Kaup and approximate long water wave equations. The explicit approximate traveling wave solutions are obtained by using this method. Here, fractional derivatives are defined in the conformable sense. The obtained traveling wave solutions are expressed by the hyperbolic, trigonometric, exponential and rational functions. Simulations of the obtained solutions are given at the end of the paper.

Keywords: The fractional Broer–Kaup equations; The fractional approximate long water wave equations; Conformable derivative; $\exp(-\phi(\xi))$ expansion method; Traveling wave solutions.

1. Introduction

Nonlinear partial differential equations are important tools used to modeled nonlinear dynamical phenomena in different fields such as mathematical biology, plasma physics, solid state physics, and fluid dynamics [1]. The traveling wave solutions of nonlinear partial differential equations play an important role in the study of nonlinear physical phenomena such as fluid dynamics, water wave mechanics, meteorology, electromagnetic theory, plasma physics and nonlinear optics etc. In the recent decade, many methods have been developed for finding the traveling wave solutions such as the Jacobi elliptic function method [2], the ansatz method [3], the exp-($\phi(\eta)$)) method [4], exp-function method [5], consistent Riccati expansion method [6], the (G'/G)-expansion method [7].

Waves have a major influence on the marine environment and ultimately on the planet climate. One of the most important and application classifications of marine waves is the shallow water wave. The shallow water equations describe the motion of water bodies wherein the depth is short relative to the scale of the waves propagating on that body and are derived from the depth-averaged Navier–Stokes equations [8]. These equations are used to describe flow in vertically well-mixed water bodies where the horizontal length scales are much greater than the fluid depth (i.e., long wavelength phenomena) and to model the hydrodynamics of lakes, estuaries, tidal flats and coastal regions, as well as deep ocean tides. The equations also, are used to study many physical phenomena such forces acting on off-shore structures and in modeling the transport of chemical species such as storm surges, tidal fluctuations and tsunami waves [9].

In the present paper, we consider space-time fractional approximate long water wave equations and Broer–Kaup equations which are used to model the bidirectional propagation of long waves in shallow water. The space-time fractional approximate long water wave equations (see, for example, [10–12]) are given in the form

$$\begin{aligned} &T_t^{\alpha}u - uT_x^{\beta}u - T_x^{\beta}v + \gamma T_x^{\beta}T_x^{\beta}u = 0,\\ &T_t^{\alpha}v - T_x^{\beta}(uv) - \gamma T_x^{\beta}T_x^{\beta}v = 0, \quad t > 0, \quad 0 < \alpha, \beta \leq 1, \end{aligned} \tag{1}$$

and the space-time fractional Broer–Kaup equations (see, for example, [13]) are given as follows

E-mail address: hcerdik@pau.edu.tr.

https://doi.org/10.1016/j.joes.2018.10.004

$$T_t^{\alpha}u + uT_x^{\beta}u + T_x^{\beta}v = 0,$$
$$T_t^{\alpha}v + T_x^{\beta}u + T_x^{\beta}(uv) + T_x^{\beta}T_x^{\beta}T_x^{\beta}u = 0,$$
$$t > 0, \quad 0 < \alpha, \beta \le 1, \tag{2}$$

Here T_t^{α} and T_x^{β} denote conformable fractional derivative with respect to t and x, respectively. These equations have been investigated in [14–17]. New exact solutions for fractional DR equation and fractional approximate long water wave equation with the modified Riemann–Liouville derivative have been obtained by using G'/G-expansion method in [14]. The time fractional coupled Boussinesq–Burger and time fractional approximate long water wave equations with conformable derivative by using the generalized Kudryashov method have been solved in [15]. The analytical approximate traveling wave solutions of time fractional Whitham–Broer–Kaup equations, time fractional coupled modified Boussinesq and time fractional approximate long wave equations have been obtained by using the coupled fractional reduced differential transform method in [16]. Here fractional derivative is defined by the Caputo sense. The fractional sub-equation method has been applied to the fractional variant Boussinesq equation and fractional approximate long water wave equation with Jumarie's modified Riemann–Liouville derivatives in [17].

2. Description of the conformable fractional derivative and its properties

For a function f: $(0, \infty) \to R$, the conformable fractional derivative of f of order $0 < \alpha < 1$ is defined as (see, for example, [18])

$$T_t^{\alpha}f(t) = \lim_{\varepsilon \to 0} \frac{f(t + \varepsilon t^{1-\alpha}) - f(t)}{\varepsilon}. \tag{3}$$

Some important properties of the conformable fractional derivative are as follows:

$$T_t^{\alpha}(af + bg)(t) = aT_t^{\alpha}f(t) + bT_t^{\alpha}g(t), \quad \forall a, b \in R, \tag{4}$$

$$T_t^{\alpha}(t^{\mu}) = \mu t^{\mu-\alpha}, \tag{5}$$

$$T_t^{\alpha}(f(g(t)) = t^{1-\alpha}g'(t)f'(g(t)). \tag{6}$$

3. Analytic solutions to the space-time fractional approximate long water wave equations

Let us consider the following transformation

$$u(x,t) = U(\xi), \quad \xi = a\frac{t^{\alpha}}{\alpha} + b\frac{x^{\beta}}{\beta}, \tag{7}$$

where a, b are constants. Substituting (7) into (1) we have the following ordinary differential equations

$$aU' - bUU' - bV' + \gamma b^2U'' = 0, \tag{8}$$

$$aV' - b(UV' + VU') - \gamma b^2V'' = 0. \tag{9}$$

Integrating (8) with respect to ξ, then we have

$$V = \frac{a}{b}U - \frac{C_1}{b} - \frac{U^2}{2} + \gamma bU'. \tag{10}$$

Substituting (10) into (9) yields

$$-\gamma^2b^3U'' + \frac{b}{2}U^3 - \frac{3a}{2}U^2 + \left(C_1 + \frac{a^2}{b}\right)U - C_2 = 0. \tag{11}$$

Here, C_1 and C_2 are integration constants. Let us suppose that the solution of (11) can be expressed in the following form:

$$U(\xi) = \sum_{i=0}^{N} a_i(\exp(-Q(\xi)))^i, \tag{12}$$

where a_i are constants to be determined later and $Q(\xi)$ satisfies the following auxiliary ordinary differential equation:

$$Q'(\xi) = \exp(-Q(\xi)) + \mu\exp(Q(\xi)) + \lambda. \tag{13}$$

Inserting (12) into (11) then by balancing the highest order derivative term and nonlinear term in result equation, the value of N can be determined as 1. Collecting all the terms with the same power of $\exp(-\phi(\xi))$, we can obtain a set of algebraic equations for the unknowns a_0, a_1, C_1, C_2, a, b:

$$-2a^2a_0 - 3aa_0^2b - a_0^3b^2 + 2C_1a_0b - 2a_1\lambda\mu b^4\gamma^2 - 2C_2b = 0;$$
$$2a_1a^2 - 6a_1aa_0b + 3a_1a_0^2b^2 - 2a_1b^4\lambda^2\gamma^2$$
$$- 4a_1\mu b^4\gamma^2 + 2C_1a_1b = 0;$$
$$3a_0a_1^2b^2 - 3aa_1^2b - 6\lambda a_1b^4\gamma^2 = 0;$$
$$a_1^3b^2 - 4a_1b^4\gamma^2 = 0.$$

Solving the algebraic equations in the Mathematica, we obtain the following set of solutions:

$$a_1 = 2b\gamma, \quad C_1 = \frac{b}{2}(a_0^2 - 2a_0b\gamma\lambda + 4b^2\gamma^2\mu),$$
$$C_2 = -\frac{b}{2}(-a_0 + b\gamma\lambda)(a_0^2 - 2a_0b\gamma\lambda + 4b^2\gamma^2\mu),$$
$$a = -b(-a_0 + b\gamma\lambda).$$

The solutions of Eq. (1) are given as follows:

$$u_i(x,t) = a_0 + 2b\gamma R_i(x,t), \tag{14}$$

$$v_i(x,t) = (a_0 - b\gamma\lambda)u_i(x,t) - \frac{u_i^2(x,t)}{2}$$
$$- \frac{1}{2}(a_0^2 - 2a_0b\gamma\lambda + 4b^2\gamma^2\mu)$$
$$- 2b^2\gamma^2(R_i^2(x,t) + \mu + \lambda R_i(x,t)), \quad i = 1, 2, 3, 4, 5. \tag{15}$$

Here $R_i(x,t)$, $i = 1, 2, 3, 4, 5$, is defined as follows:

When $\lambda^2 - 4\mu > 0$, $\mu \neq 0$,

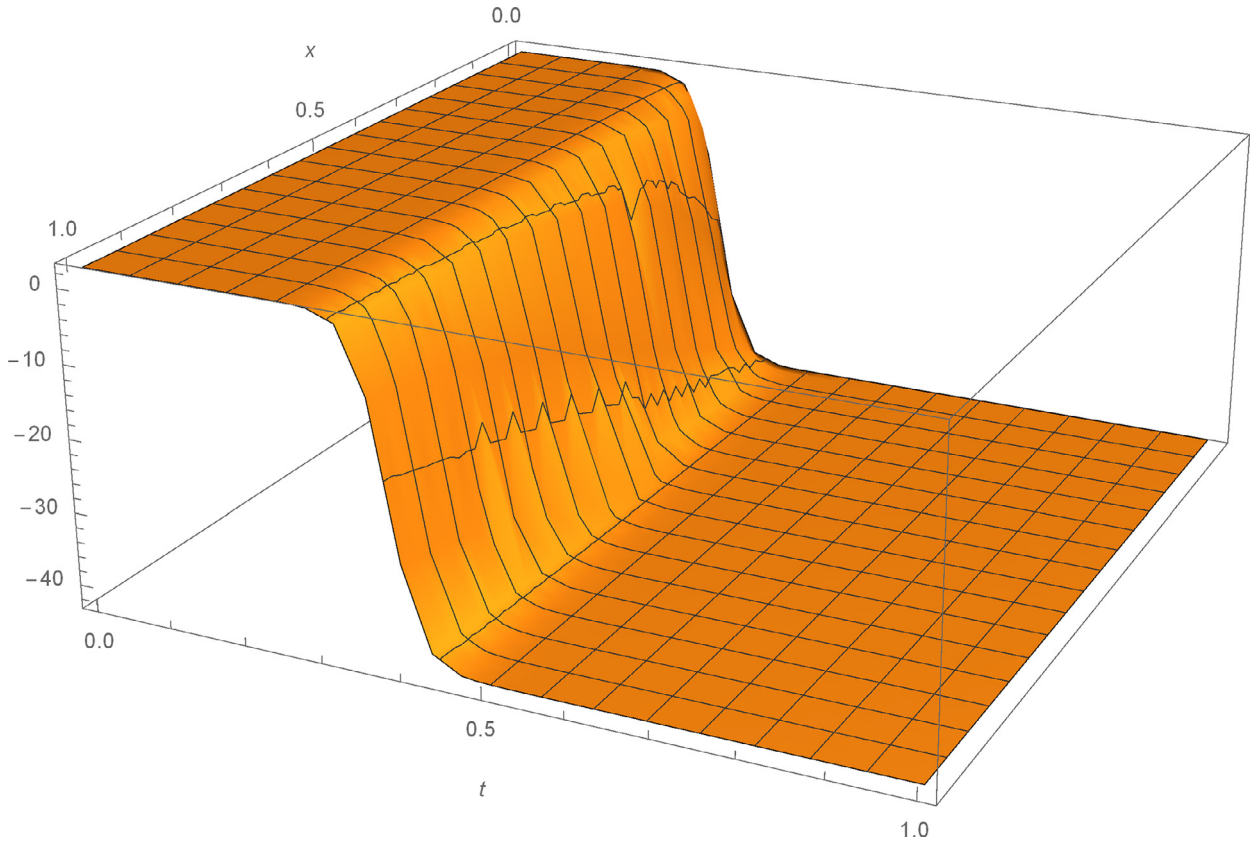

Fig. 1. 3D plot of the solitary wave solution $u_1(x,\ t)$ of Eq. (1) for $a_0 = 10, b = 1, \mu = 1, C = 10, \lambda = 3, \gamma = 10,\ \ \alpha = 0.75,\ \ \beta = 0.5$.

$$R_1(x,t) = \frac{2\mu}{-\lambda - \sqrt{\lambda^2 - 4\mu}\tanh(\frac{\sqrt{\lambda^2-4\mu}}{2}(b(a_0 - b\gamma\lambda)\frac{t^\alpha}{\alpha} + b\frac{x^\beta}{\beta} + C))}, \tag{16}$$

When $\lambda^2 - 4\mu < 0,\ \ \mu \neq 0,$

$$R_2(x,t) = \frac{2\mu}{-\lambda + \sqrt{4\mu - \lambda^2}\tan\left(\frac{\sqrt{4\mu-\lambda^2}}{2}(b(a_0 - b\gamma\lambda)\frac{t^\alpha}{\alpha} + b\frac{x^\beta}{\beta} + C)\right)} \tag{17}$$

When $\lambda^2 - 4\mu > 0,\ \ \mu = 0,\ \ \lambda \neq 0,$

$$R_3(x,t) = \frac{\lambda}{\cosh(b(a_0 - b\gamma\lambda)\frac{t^\alpha}{\alpha} + b\frac{x^\beta}{\beta} + C) + \sinh(b(a_0 - b\gamma\lambda)\frac{t^\alpha}{\alpha} + b\frac{x^\beta}{\beta} + C) - 1}.$$

When $\lambda^2 - 4\mu = 0,\ \ \mu \neq 0,\ \ \lambda \neq 0,$

$$R_4(x,t) = -\frac{\lambda^2(b(a_0 - b\gamma\lambda)\frac{t^\alpha}{\alpha} + b\frac{x^\beta}{\beta} + C)}{2\lambda(b(a_0 - b\gamma\lambda)\frac{t^\alpha}{\alpha} + b\frac{x^\beta}{\beta} + C) + 4}. \tag{18}$$

When $\lambda^2 - 4\mu = 0,\ \ \mu = 0,\ \ \lambda = 0,$

$$R_5(x,t) = \frac{1}{(b(a_0 - b\gamma\lambda)\frac{t^\alpha}{\alpha} + b\frac{x^\beta}{\beta} + C)}. \tag{19}$$

Here C is the integration constant.

Figs. 1–4 represent the change of amplitude and nature of the solitary waves for each obtained solitary wave solutions. The solutions $u_1(x,\ t)$, $u_2(x,\ t)$ and $v_1(x,\ t)$ of Eq. (1) are simulated as traveling wave solutions for various values of the physical parameters in Figs. 1–4. Figs. 1 and 2 show solitary wave solutions of Eq. (1). 3D plots of the obtained solutions $u_1(x,\ t)$ and $v_1(x,\ t)$ are given in Fig. 1 and Fig. 2 for parameters $a_0 = 10, b = 1, \mu = 1, C = 10, \lambda = 3, \gamma = 10,\ \ \alpha = 0.75,\ \ \beta = 0.5$, respectively. Figs. 3 and 4 are kink-type periodic wave solutions of Eq. (1). 3D plot of the obtained solution $u_2(x,\ t)$ is given for parameters $a_0 = 0.5, b = 1, \mu = 1, C = 5, \lambda = 1, \gamma = 1\ \ \alpha = 0.75,\ \ \beta = 0.5$ in Fig. 3. Fig. 4 demonstrates the same solution with 2D plot for $0 \leq x \leq 50$ at $t = 1$.

4. Analytic solutions to the space-time fractional Broer–Kaup equations

Applying the transformation (7) into (2) we have the following ordinary differential equations

$$aU' + bUU' + bV' = 0, \tag{20}$$

$$aV' + bU' + b(UV' + VU') + b^3U''' = 0. \tag{21}$$

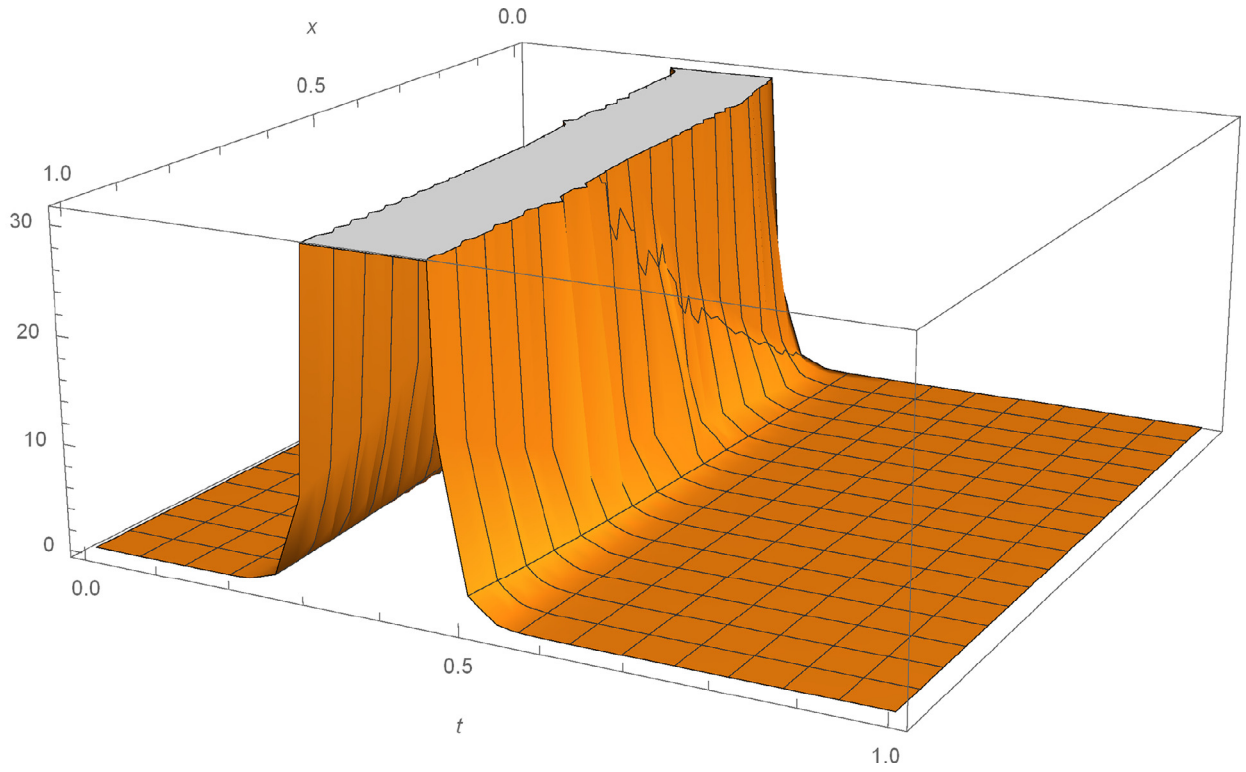

Fig. 2. 3D plot of the solitary wave solution $v_1(x, t)$ of Eq. (1) for $a_0 = 10, b = 1, \mu = 1, C = 10, \lambda = 3, \gamma = 10, \quad \alpha = 0.75, \quad \beta = 0.5$.

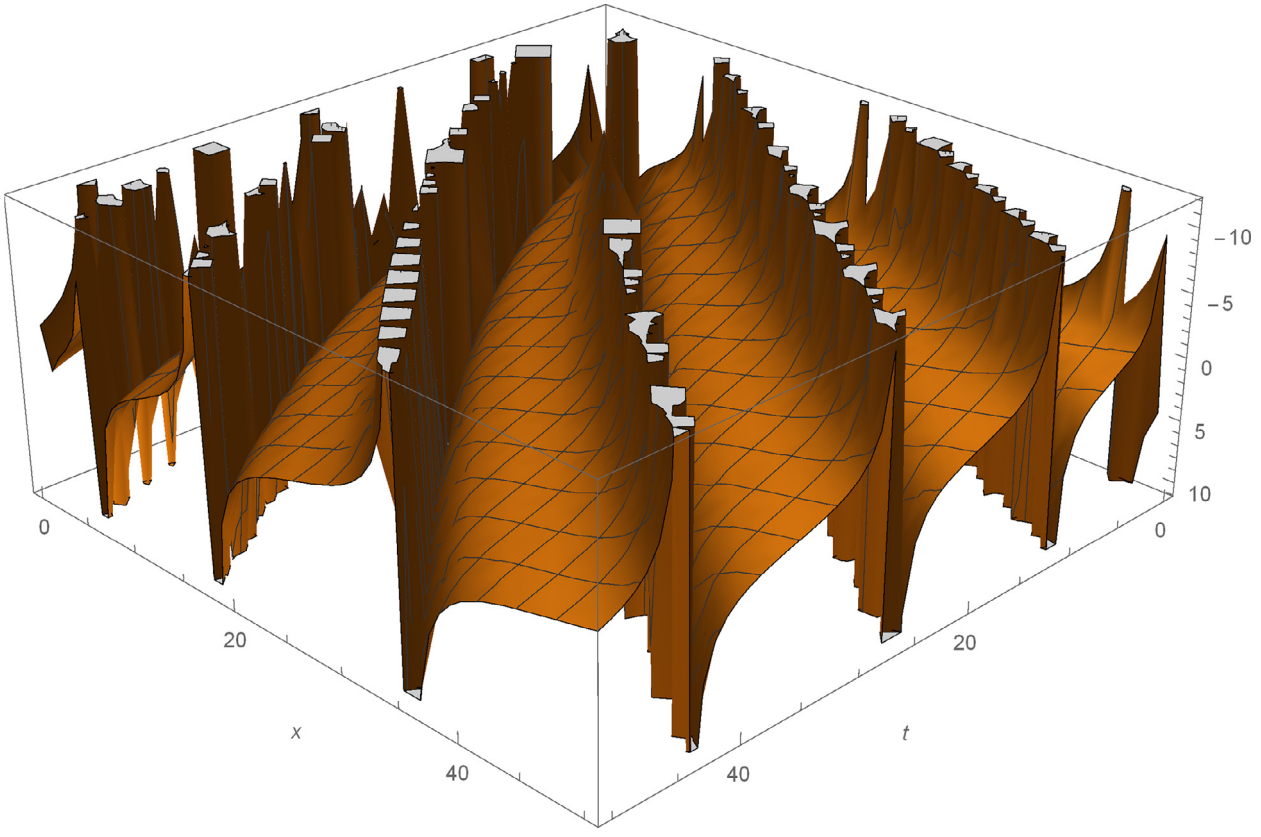

Fig. 3. 3D plot of the periodic wave solution $u_2(x, t)$ of Eq. (1) for $a_0 = 0.5, b = 1, \mu = 1, C = 5, \lambda = 1, \gamma = 1, \quad \alpha = 0.75, \quad \beta = 0.5$.

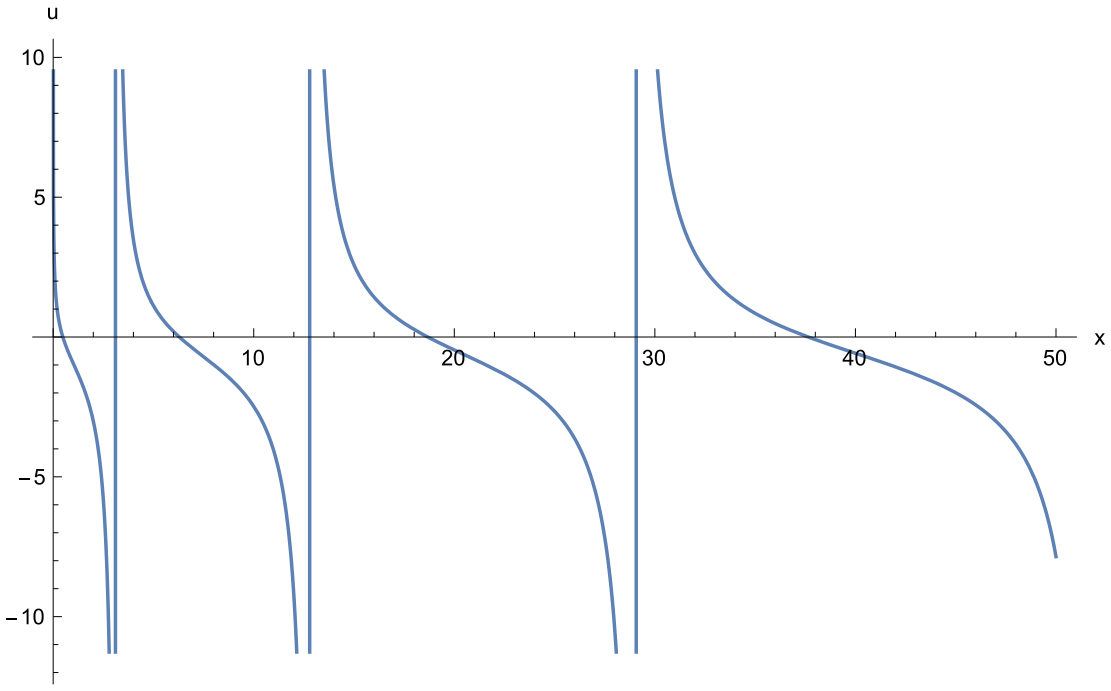

Fig. 4. 2D plot of the periodic wave solution $u_2(x, 1)$ of Eq. (1) for $a_0 = 0.5, b = 1, \mu = 1, C = 5, \lambda = 1, \gamma = 1, \ \alpha = 0.75, \ \beta = 0.5$.

Integrating (20) with respect to ξ, then we have

$$V = \frac{C_1}{b} - \frac{U^2}{2} - \frac{a}{b}U. \tag{22}$$

Substituting (22) into (21) yields

$$b^3U'' - \frac{b}{2}U^3 - \frac{3a}{2}U^2 + \left(C_1 + b - \frac{a^2}{b}\right)U - C_2 = 0. \tag{23}$$

Here C_1 and C_2 are integration constants. Let us suppose that the solution of (23) can be expressed in the form (12). Inserting (12) into (23) and balancing the highest order derivative term and nonlinear term in result equation, the value of N can be determined as 1. Collecting all the terms with the same power of $\exp(-\phi(\xi))$, we can obtain a set of algebraic equations for the unknowns a_0, a_1, C_2, C_2, a, b:

$$\begin{aligned}
&-2a^2a_0 - 3aa_0^2b - a_0^3b^2 + 2a_0b^2 + 2C_1a_0b \\
&+ 2a_1\lambda\mu b^4 - 2C_2b = 0; \\
&-2a_1a^2 - 6a_1aa_0b - 3a_1a_0^2b^2 + 2a_1b^4\lambda^2 \\
&+ 4a_1\mu b^4 + 2a_1b^2 + 2C_1a_1b = 0; \\
&-3a_0a_1^2b^2 - 3aa_1^2b + 6\lambda a_1b^4 = 0; \\
&-a_1^3b^2 + 4a_1b^4 = 0;
\end{aligned}$$

Solving the algebraic equations in the Mathematica, we obtain the following set of solutions:

$$R_3(x,t) = \frac{\lambda}{\cosh(b(-a_0 + b\lambda)\frac{t^\alpha}{\alpha} + b\frac{x^\beta}{\beta} + C) + \sinh(b(-a_0 + b\lambda)\frac{t^\alpha}{\alpha} + b\frac{x^\beta}{\beta} + C) - 1}.$$

$$a_1 = 2b, \quad C_1 = -\frac{b}{2}(2 + a_0^2 - 2a_0b\lambda + 4b^2\mu),$$

$$C_2 = \frac{b}{2}(-a_0 + b\lambda)(a_0^2 - 2a_0b\lambda + 4b^2\mu), \quad a = b(-a_0 + b\lambda).$$

The solutions of Eq. (1) are given as follows:

$$u_i(x,t) = a_0 + 2bR_i(x,t), \tag{24}$$

$$\begin{aligned}
v_i(x,t) = {} & \frac{-1}{2}(2 + a_0^2 - 2a_0b\lambda + 4b^2\mu) - \frac{u_i^2(x,t)}{2} \\
& + (a_0 - b\lambda)u_i(x,t) \quad i = 1, 2, 3, 4, 5.
\end{aligned} \tag{25}$$

Here $R_i(x,t), i = 1, 2, 3, 4, 5$, is defined as follows:

When $\lambda^2 - 4\mu > 0, \quad \mu \neq 0,$

$$R_1(x,t) = \frac{2\mu}{-\lambda - \sqrt{\lambda^2 - 4\mu}\tanh(\frac{\sqrt{\lambda^2-4\mu}}{2}(b(-a_0 + b\lambda)\frac{t^\alpha}{\alpha} + b\frac{x^\beta}{\beta} + C))}, \tag{26}$$

When $\lambda^2 - 4\mu < 0, \quad \mu \neq 0,$

$$R_2(x,t) = \frac{2\mu}{-\lambda + \sqrt{4\mu - \lambda^2}\tan(\frac{\sqrt{4\mu-\lambda^2}}{2}(b(-a_0 + b\lambda)\frac{t^\alpha}{\alpha} + b\frac{x^\beta}{\beta} + C))} \tag{27}$$

When $\lambda^2 - 4\mu > 0, \quad \mu = 0, \quad \lambda \neq 0,$

When $\lambda^2 - 4\mu = 0, \quad \mu \neq 0, \quad \lambda \neq 0,$

$$R_4(x,t) = -\frac{\lambda^2(b(-a_0 + b\lambda)\frac{t^\alpha}{\alpha} + b\frac{x^\beta}{\beta} + C)}{2\lambda(b(-a_0 + b\lambda)\frac{t^\alpha}{\alpha} + b\frac{x^\beta}{\beta} + C) + 4}. \tag{28}$$

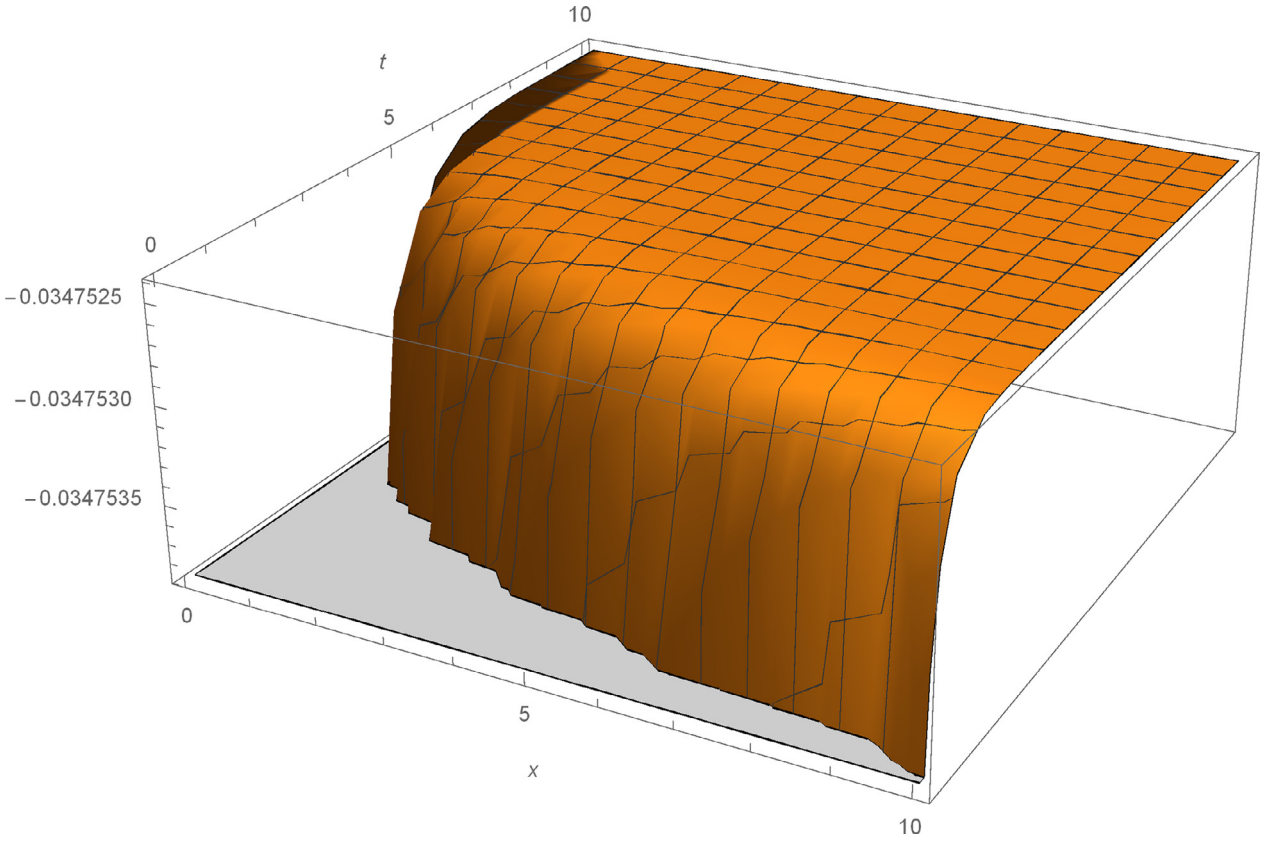

Fig. 5. 3D plot of the solitary wave solution $u_1(x,\ t)$ of Eq. (2) for $a_0 = 0.5, b = 0.7, \mu = 1, C = 1, \lambda = 3,\ \ \alpha = 0.75,\ \ \beta = 0.5$.

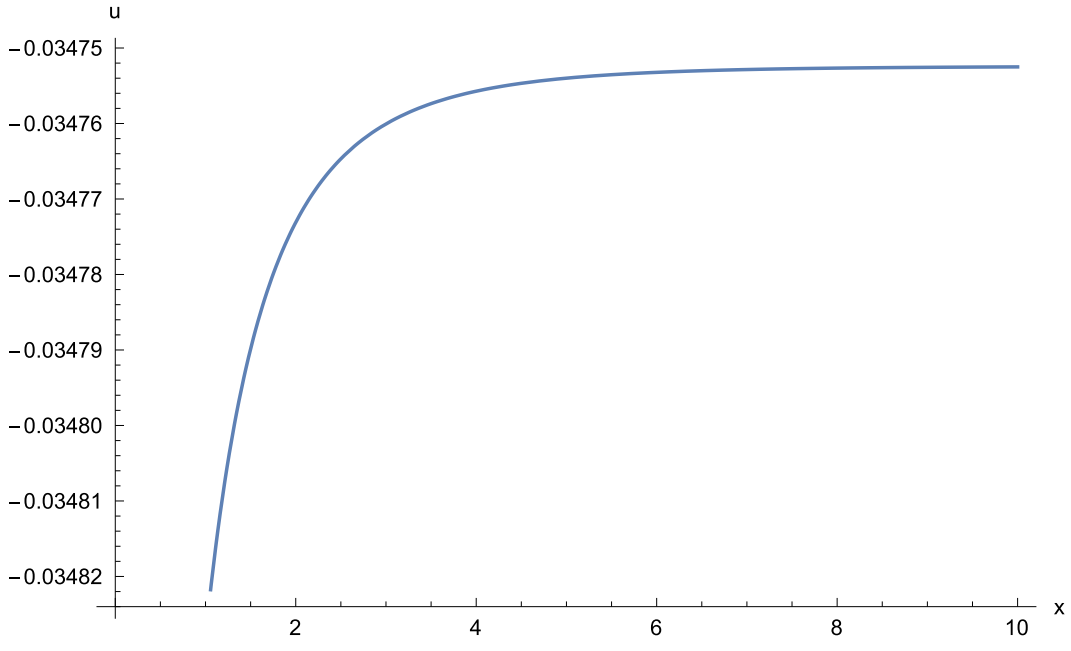

Fig. 6. 2D plot of the solitary wave solution $u_1(x,\ 1)$ of Eq. (2) for $a_0 = 0.5, b = 0.7, \mu = 1, C = 1, \lambda = 3,\ \ \alpha = 0.75,\ \ \beta = 0.5$.

When $\lambda^2 - 4\mu = 0,\ \ \mu = 0,\ \ \lambda = 0,$

$$R_5(x,t) = \frac{1}{(b(-a_0 + b\lambda)\frac{t^\alpha}{\alpha} + b\frac{x^\beta}{\beta} + C)}. \tag{29}$$

The solutions $u_1(x,\ t)$, $v_2(x,\ t)$ and $v_3(x,\ t)$ of Eq. (2) are simulated as traveling wave solutions for various values of the physical parameters in Figs. 5–9. Figs. 5 and 6 show solitary wave solutions of Eq. (2). 3D plot of the obtained solution $u_1(x,\ t)$ is given for $a_0 = 0.5, b = 0.7, \mu = 1, C =$

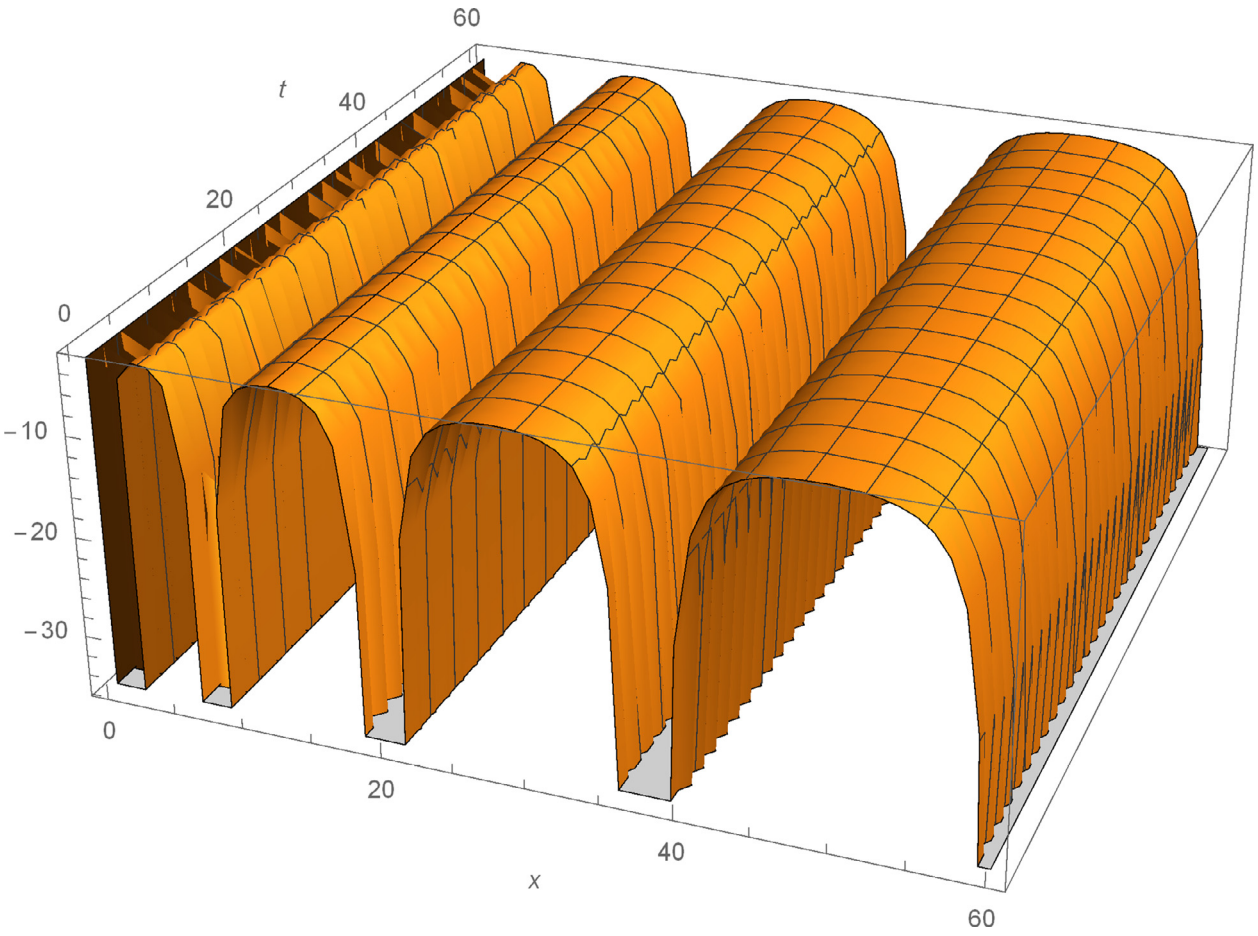

Fig. 7. 3D plot of the periodic wave solution $v_2(x,\ t)$ of Eq. (2) for $a_0 = 0.5, b = 0.7, \mu = 2, C = 1, \lambda = 1,\ \ \alpha = 0.75,\ \ \beta = 0.5$.

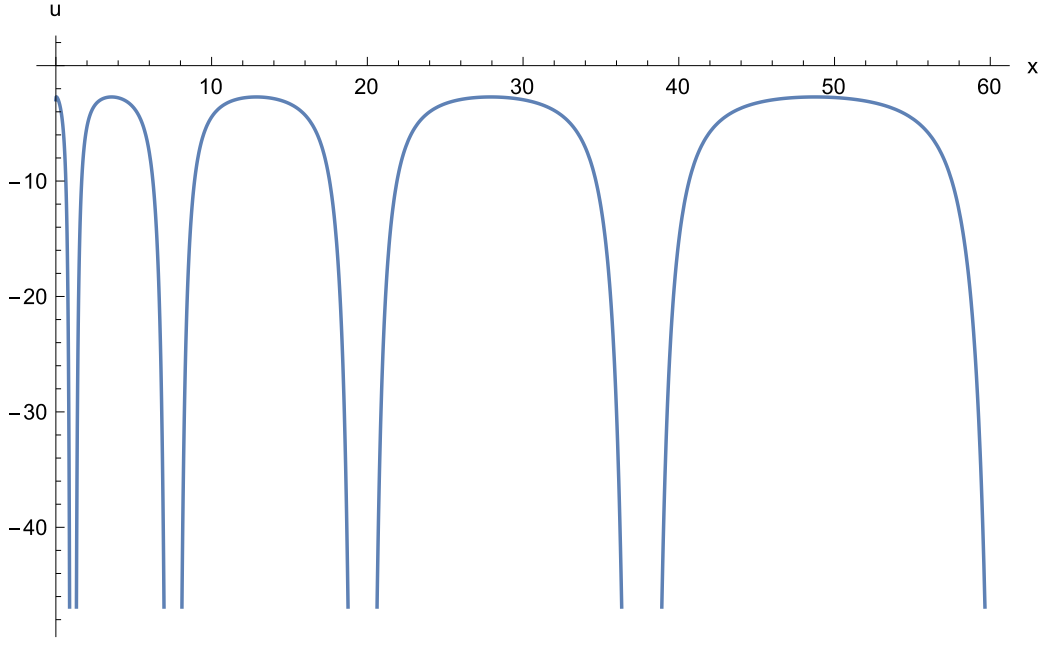

Fig. 8. 2D plot of the periodic wave solution $v_2(x,\ 1)$ of Eq. (2) for $a_0 = 0.5, b = 0.7, \mu = 2, C = 1, \lambda = 1,\ \ \alpha = 0.75,\ \ \beta = 0.5$.

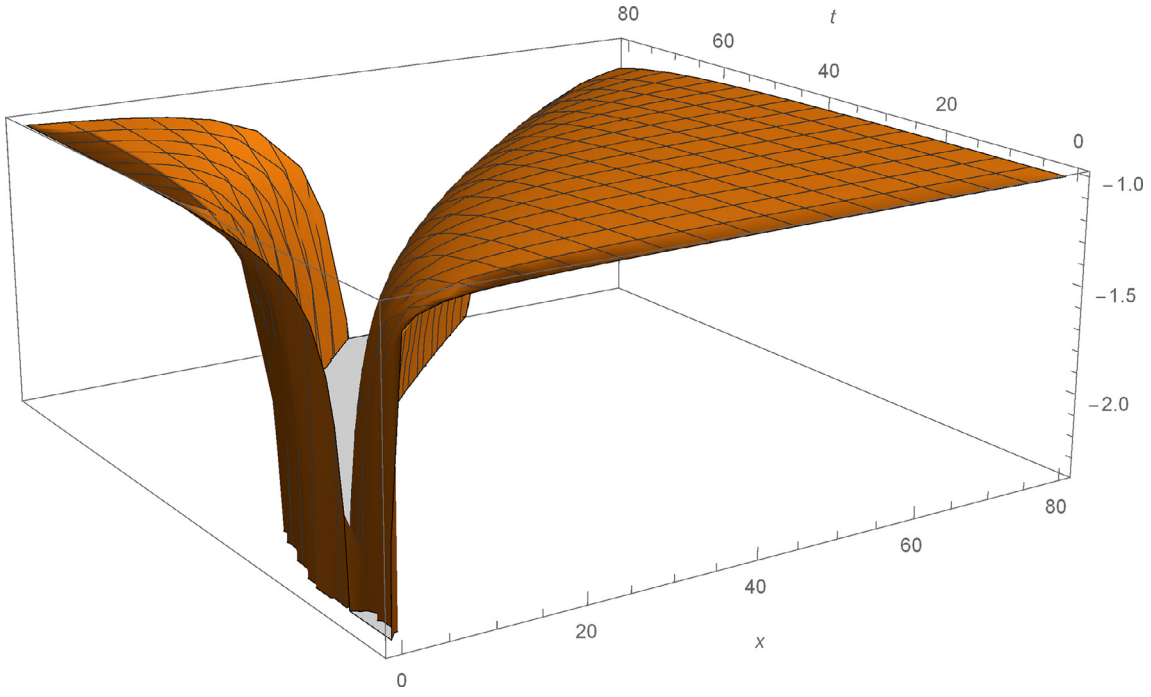

Fig. 9. 3D plot of the solitary wave solution $v_3(x,\ t)$ of Eq. (2) for $a_0 = 0.5, b = 0.7, \mu = 0, C = 1, \lambda = 0.1,\ \ \alpha = 0.75,\ \ \beta = 0.5$.

$1, \lambda = 3,\ \ \alpha = 0.75,\ \ \beta = 0.5$. Fig. 6 also illustrates the same solution with 2D plot for $0 \leq x \leq 10$ at $t = 1$. Figs. 7 and 8 show periodic wave solutions of Eq. (2). 3D and 2D plots of the obtained solution $v_2(x,\ t)$ and $v_2(x,\ 1)$ are given for $a_0 = 0.5, b = 0.7, \mu = 2, C = 1, \lambda = 1,\ \ \alpha = 0.75,\ \ \beta = 0.5$, respectively. From Fig. 8, we can see that the wave amplitudes go to infinity and the wavelengths increase when x approaches to infinity. Fig. 9 shows solitary wave solution $v_3(x,\ t)$ of Eq. (2). 3D plot of the obtained solution $v_3(x,\ t)$ is given for $a_0 = 0.5, b = 0.7, \mu = 0, C = 1, \lambda = 0.1,\ \ \alpha = 0.75,\ \ \beta = 0.5$. Note that the 3D graphs describe the behavior of u and v in space x at time t, which represents the change of amplitude and shape for each obtained solitary wave solutions. 2D graphs describe the behavior of u and v in space x at fixed time $t = 1$. All graphics in figures are drawn by the aid of Mathematica 10.

5. Conclusion

In the present paper, the space and time fractional Broer–Kaup and approximate long water wave equations with the conformable fractional derivative are considered. By using the $\exp(-\phi(\xi))$ expansion method new approximate analytic solutions are obtained. The new analytical solutions obtained in this paper have not been reported in the literature so far. This method is useful in solving wide classes of conformable nonlinear fractional differential equations.

References

[1] M. Duranda, D. Langevin, Eur. Phys. J. E 7 (2002) 35–44.
[2] A.H. Bhrawy, M.A. Abdelkawy, E.M. Hilal, A.A. Alshaery, A. Biswas, Appl. Math. Inf. Sci. 8 (2014) 2119–2128.
[3] L. Song, H. Zhang, Appl. Math. Comput. 180 (2006) 664–675.
[4] M.M. Hossain, H. Roshid, M.A.N. Sheikh, J. Found. Appl. Phys. 3 (2016) 1–13.
[5] A.G. Davodi, D.D. Ganji, A.G. Davodi, A. Asgari, Appl. Math. Comput. 217 (2010) 1415–1420.
[6] Y. Jiang, D. Xian, Z. Dai, Therm. Sci. 21 (2017) 1783–1788.
[7] G. Ebadi, A. Biswas, J. Frankl. Inst. 347 (2010) 1391–1398.
[8] C.M. Szpilka, R.L. Kolar, Adv. Water Resour. 26 (2003) 649–662.
[9] J. Shin, J. Tang, M.N. Wu, Acta Mech. Sin. 24 (2008) 523–532.
[10] L.J.F. Broer, Appl. Sci. Res. 31 (1975) 377–395.
[11] G.B. Whitham, Proc. R. Soc. Lond. A Math. Phys. Sci. 299 (1967) 6–25.
[12] M. Wang, J. Zhang, X. Li, Appl. Math. Comput. 206 (2008) 321–326.
[13] D.J. Kaup, Prog. Theor. Phys. 54 (1975) 396–408.
[14] O. Guner, H. Atik, A.A. Kayyrzhanovich, Optik 130 (2017) 696–701.
[15] M.M.A. Khater, D. Kumar, JOES 2 (2017) 223–228.
[16] S.S. Ray, Math. Meth. Appl. Sci. 38 (2015) 352–1368.
[17] L. Yan, Int. J. Numer. Method. H 25 (2015) 33–40.
[18] R. Khalil, M.A. Horani, A. Yousef, M. Sababheh, J. Comput. Appl. Math. 264 (2014) 65–70.